LETTER

doi:10.1038/nature12805

Role of Tet1 in erasure of genomic imprinting

Shinpei Yamaguchi[1,2,3], Li Shen[1], Yuting Liu[1,2,3], Damian Sendler[1] & Yi Zhang[1,2,3,4,5]

Genomic imprinting is an allele-specific gene expression system that is important for mammalian development and function[1]. The molecular basis of genomic imprinting is allele-specific DNA methylation[1,2]. Although it is well known that the *de novo* DNA methyltransferases Dnmt3a and Dnmt3b are responsible for the establishment of genomic imprinting[3], how the methylation mark is erased during primordial germ cell (PGC) reprogramming remains unclear. Tet1 is one of the ten-eleven translocation family proteins, which have the capacity to oxidize 5-methylcytosine (5mC)[4–6], specifically expressed in reprogramming PGCs[7]. Here we report that Tet1 has a critical role in the erasure of genomic imprinting. We show that despite their identical genotype, progenies derived from mating between *Tet1* knockout males and wild-type females exhibit a number of variable phenotypes including placental, fetal and postnatal growth defects, and early embryonic lethality. These defects are, at least in part, caused by the dysregulation of imprinted genes, such as *Peg10* and *Peg3*, which exhibit aberrant hypermethylation in the paternal allele of differential methylated regions (DMRs). RNA-seq reveals extensive dysregulation of imprinted genes in the next generation due to paternal loss of Tet1 function. Genome-wide DNA methylation analysis of embryonic day 13.5 PGCs and sperm of *Tet1* knockout mice revealed hypermethylation of DMRs of imprinted genes in sperm, which can be traced back to PGCs. Analysis of the DNA methylation dynamics in reprogramming PGCs indicates that Tet1 functions to wipe out remaining methylation, including imprinted genes, at the late reprogramming stage. Furthermore, we provide evidence supporting the role of Tet1 in the erasure of paternal imprints in the female germ line. Thus, our study establishes a critical function of Tet1 in the erasure of genomic imprinting.

The dynamic expression pattern of Tet1 in PGCs makes it a primary candidate for imprinting erasure[7]. To test this possibility, we generated paternal knockout mice (paternal^{KO}; progenies from *Tet1*$^{-/-}$ male × wild-type female mice) and analysed the effect of paternal Tet1 functional loss on the development of the next generation based on the idea that imprinting defects affect the next generation[1,2]. Unlike the meiotic defects in the oocytes of *Tet1* knockout females[7], *Tet1* knockout testes are morphologically and functionally normal, which makes the generation of paternal^{KO} progeny possible. We found that *Tet1* paternal^{KO} pups show great variability in body size when compared to controls (progeny from *Tet1*$^{+/-}$ male × wild-type female mice) (Fig. 1a, b). In addition, the placental sizes of paternal^{KO} mice are significantly smaller than that of controls (Fig. 1c). Placental size positively correlates with body size ($R = 0.69$) in paternal^{KO} pups, indicating that the growth retardation of the embryos is probably caused by the developmental failure of the placenta, which is already noticeable at embryonic day (E)13.5 and E16.5 (Extended Data Fig. 1a, b). Furthermore, we found that about half of paternal^{KO} pups die within 3 days of birth (Extended Data Fig. 1c). Moreover, about half of survived pups showed marked growth retardation (Fig. 1d, e). This unusually large variation in body size persists to adulthood (Extended Data Fig. 1d).

In addition to growth defects, we found that the litter size of paternal^{KO} mice is also greatly reduced compared to the control crosses (Fig. 2a and Extended Data Fig. 1e). To examine potential embryonic developmental defects of *Tet1* paternal^{KO} pups, we dissected embryos at E13.5 and noticed some absorbed embryos *in utero* (36.4%, $n = 33$ from 4 litters of paternal^{KO}; 2.8%, $n = 36$ from 5 litters of control) (Extended Data Fig. 1f). Although no absorbed embryos were observed at E10.5, about 33.3% ($n = 48$ from 6 litters) of paternal^{KO} embryos exhibited developmental abnormalities, particularly in posterior parts, and no clear somites were observed (Fig. 2b and Extended Data Fig. 1g). Although all of the E9.5 paternal^{KO} embryos analysed were morphologically normal, some

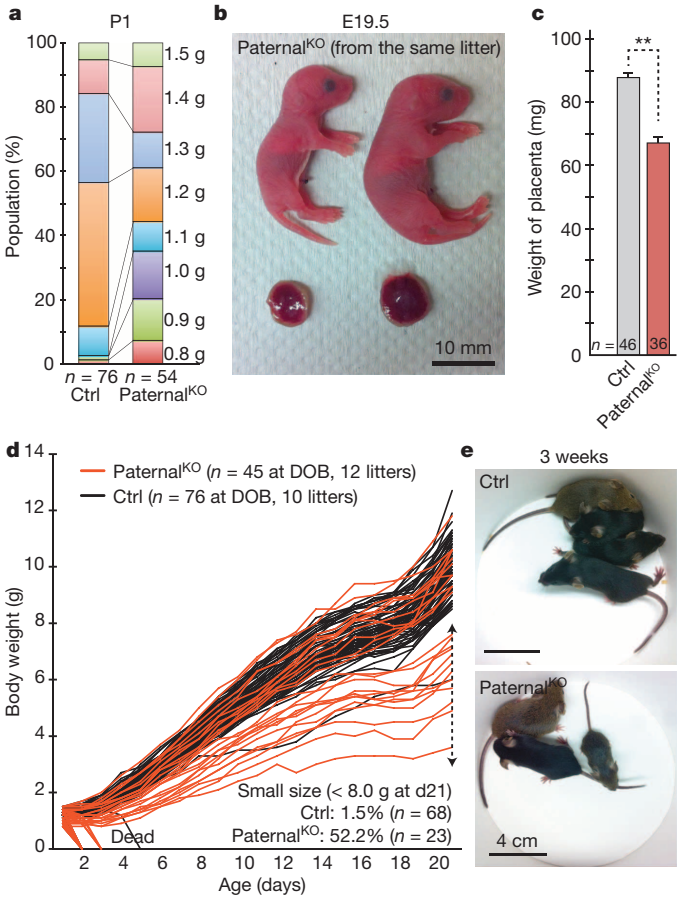

Figure 1 | *Tet1* paternal knockout results in fetal and postnatal growth defects. **a**, Increased variation of body weight at birth in *Tet1* paternal^{KO} pups. Note that pups with weight <1.2 g or >1.3 g account for most of the population in *Tet1* paternal^{KO} mice, whereas most of the control pups are between 1.2–1.3 g at birth. **b**, Representative image of paternal^{KO} pups from the same litter showing big variation in body and placental sizes. Embryos and their placentae were recovered by Caesarean section at the day of birth (E19.5). **c**, Average placental weights at E19.5. Error bars indicate s.e.m. $^{**}P < 0.01$. **d**, Growth curves of individual pups. The lines that drop to zero indicate mice that were found dead at the time indicated. **e**, Representative image of 3-week-old litters from control and paternal^{KO} mice.

[1]Howard Hughes Medical Institute, Boston Children's Hospital, Boston, Massachusetts 02115, USA. [2]Program in Cellular and Molecular Medicine, Boston Children's Hospital, Boston, Massachusetts 02115, USA. [3]Division of Hematology/Oncology, Department of Pediatrics, Boston Children's Hospital, Boston, Massachusetts 02115, USA. [4]Department of Genetics, Harvard Medical School, Boston, Massachusetts 02115, USA. [5]Harvard Stem Cell Institute, WAB-149G, 200 Longwood Avenue, Boston, Massachusetts 02115, USA.

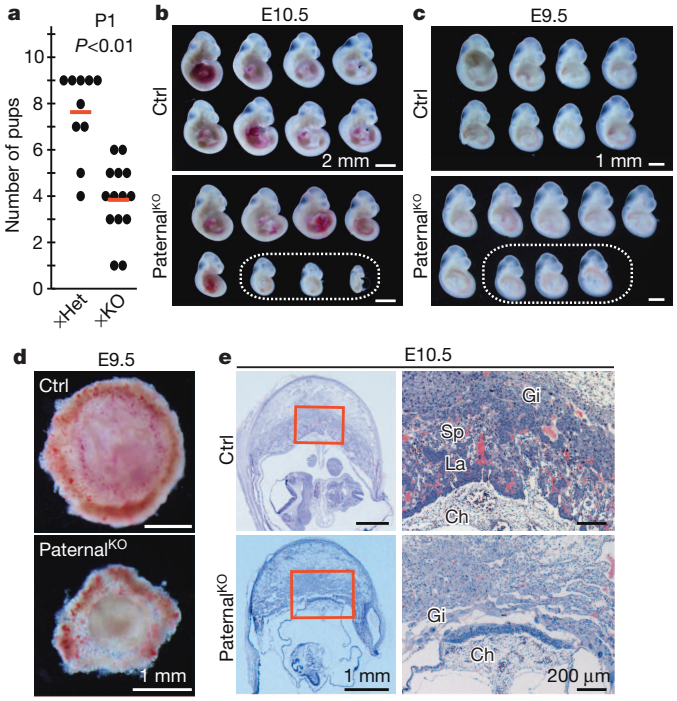

Figure 2 | Early embryonic lethality caused by placental defects in *Tet1* paternal knockout mice. **a**, Mating scores of $Tet1^{+/-}$ male × wild-type female (×Het) and $Tet1^{-/-}$ male × wild-type female (×KO) mice. Black dots indicate the numbers of pups in each litter at the day of birth. Red lines indicate the mean litter size. **b**, E10.5 embryos recovered from a single litter of control and paternal^{KO} mice. The dotted oval indicates morphologically abnormal embryos. **c**, E9.5 embryos recovered from a single litter of control and paternal^{KO} mice. The dotted oval indicates small embryos whose placentae were morphologically abnormal. **d**, Representative images of E9.5 placentae. **e**, Representative images of haematoxylin and eosin staining of E10.5 placentae. Red rectangles indicate the enlarged regions shown in the right panels. Ch, chorionic plate; Gi, trophoblast giant cells; La, labyrinthine zone; Sp, spongioblast.

of them were smaller and had abnormal placentae (34.6%, $n = 26$ from 3 litters) (Fig. 2c, d and Extended Data Fig. 1h). Histological analysis of E9.5 and E10.5 paternal^{KO} placentae revealed a lack of chorionic plate extension and a defect in labyrinthine zone development (Fig. 2e and Extended Data Fig. 1i). Because the frequency of placental abnormality at E9.5 is similar to the frequency of embryo absorption at E13.5, it is likely that the placental defect is one of the major causes of embryonic lethality and reduced litter size of paternal^{KO} embryos. Collectively, the above analyses revealed that loss of Tet1 function in the paternal germ line results in a set of phenotypes that include: (1) early embryonic lethality; (2) placental and embryonic growth defects; and (3) postnatal growth retardation (Extended Data Fig. 1j).

Previous studies have established a critical function of some imprinted genes in embryonic and placental development[1,8]. The phenotypic similarity between *Tet1* paternal^{KO} mice and *Peg10* knockout mice prompted us to examine whether paternal functional loss of Tet1 results in dysregulation of *Peg10* in the paternal^{KO} embryos[9]. Quantitative reverse transcription PCR (qRT–PCR) analysis revealed loss of *Peg10* expression in 33.3% of paternal^{KO} E9.5 embryos ($n = 30$ from 4 litters) (Fig. 3a). In contrast, all of the embryos from controls showed normal *Peg10* expression ($n = 13$ from 2 litters) (data not shown). *Sgce*, a neighbouring imprinted gene of *Peg10*, was simultaneously downregulated in *Peg10*-dysregulated paternal^{KO} embryos (Fig. 3b), indicating co-regulation of these two imprinted genes.

To reveal additional imprinted genes affected by Tet1 deletion, we performed RNA-seq analysis on 10 paternal^{KO} and 3 control E9.5 embryos (Supplementary Table 1). We found that 11–46 out of 81 expressed imprinted genes were dysregulated (fold change (FC) >1.5) in each paternal^{KO} embryo analysed (Fig. 3c and Supplementary Table 2). The dysregulated genes include imprinting gene clusters such as *Mest–Copg2*, *Peg10–Sgce*, *Zim1–Peg3–Usp29*, *Kcnq1ot1–Cdkn1c*, *Ddc–Grb10* and *Impact* (Fig. 3d and Extended Data Fig. 2a, c). Notably, we observed upregulation of maternally expressed genes and downregulation of paternally expressed genes in individual *Tet1* paternal^{KO} embryos (Extended Data Fig. 2b and Supplementary Table 2), indicating that maternalization of the paternal allele of imprinted gene expression pattern is a common phenomenon in *Tet1* paternal^{KO} embryos. In addition to imprinted genes, RNA-seq also identified 1,540 genes for which expression was markedly altered (905 upregulated and 635 downregulated, FC >1.5) in at least two of the ten paternal^{KO} embryos analysed (Extended Data Fig. 3 and Supplementary Table 3). Considering the fact that the paternal^{KO} and half of control embryos have the same heterozygous *Tet1* genotype, many of the gene expression changes are probably caused by either the changes in imprinted gene expression or the consequences of the phenotypes, and not simply an effect of the genotype.

To confirm that dysregulation of imprinted genes is indeed linked to perturbation of DNA methylation, we performed conventional bisulphite sequencing (BS-seq). Whereas the *Peg10* DMR was methylated to ~50% in controls, the DMR is almost fully methylated in *Peg10*-dysregulated *Tet1* paternal^{KO} embryos (Fig. 3e). These data are consistent with previous findings that *Peg10* and *Sgce* are specifically expressed from the unmethylated paternal allele and are silenced at the methylated maternal allele[10]. Thus, our data support the notion that hypermethylation of the paternal allele leads to silencing of *Peg10*, which causes early embryonic lethality of paternal^{KO} embryos through placental malfunction. Similar analysis also revealed hypermethylation of the *Air–Igf2r* cluster and *Impact* loci in *Air–Igf2r*- and *Impact*-dysregulated paternal^{KO} embryos, respectively (Extended Data Fig. 4a–d), further confirming the relationship between DMR hypermethylation and altered imprinted gene expression in *Tet1* paternal^{KO} embryos.

Normal expression of imprinted genes is critical for placental development and fetal growth[8]. To examine whether the growth defects observed in paternal^{KO} embryos are caused by imprinting defects in the placenta, we analysed gene expression in E19.5 paternal^{KO} placentae. qRT–PCR analysis showed that several imprinted genes are dysregulated in smaller placentae of paternal^{KO} mice (Extended Data Fig. 4e, numbers 4–7). The expression level of *Igf2r* in placentae of paternal^{KO} mice numbers 4–6 is about twice as much as that in control, indicating biallelic expression. Similarly, *Peg3*, *Usp29* and *Zim1* are concurrently dysregulated in the placenta of paternal^{KO} number 7. Furthermore, BS-seq analysis revealed that *Peg3* DMR is hypermethylated in *Peg3*-negative placentae of paternal^{KO} mice (Extended Data Fig. 4f). These data indicate that imprinting of the paternal allele at these loci is maternalized, which probably accounts for the placental developmental defects.

The maternalization in imprinted gene expression and DMR methylation of the paternal allele in paternal^{KO} embryos and placentae prompted us to ask whether the aberrant DNA methylation pattern originates from the sperm genome of *Tet1* knockout males. To this end, we performed BS-seq analysis, which revealed that part of the *Peg10* DMR remains methylated in *Tet1* knockout sperm, whereas the same region is nearly completely demethylated in the control sperm (Extended Data Fig. 4g).

To determine whether hypermethylation of imprinted DMRs is a general phenomenon in the *Tet1* knockout germ line, we performed global DNA methylation analysis of E13.5 male PGCs and sperm by reduced representative bisulphite sequencing (RRBS) (Extended Data Fig. 5a, b and Supplementary Table 4). Consistent with our previous report[7], no global change in DNA methylation levels was observed in E13.5 PGCs or sperm (Fig. 4a, b). However, the analysis identified 2,608 (6.8% of commonly covered sites (that is, sites having enough reads of RRBS analysis in both E13.5 PGCs and sperm)) and 422 (1.1% of commonly covered sites) hypermethylated sites in *Tet1* knockout PGCs and sperm, respectively (Supplementary Tables 5 and 6). Among the 422 hypermethylated sites in *Tet1* knockout sperm, 348 (82.5%) of

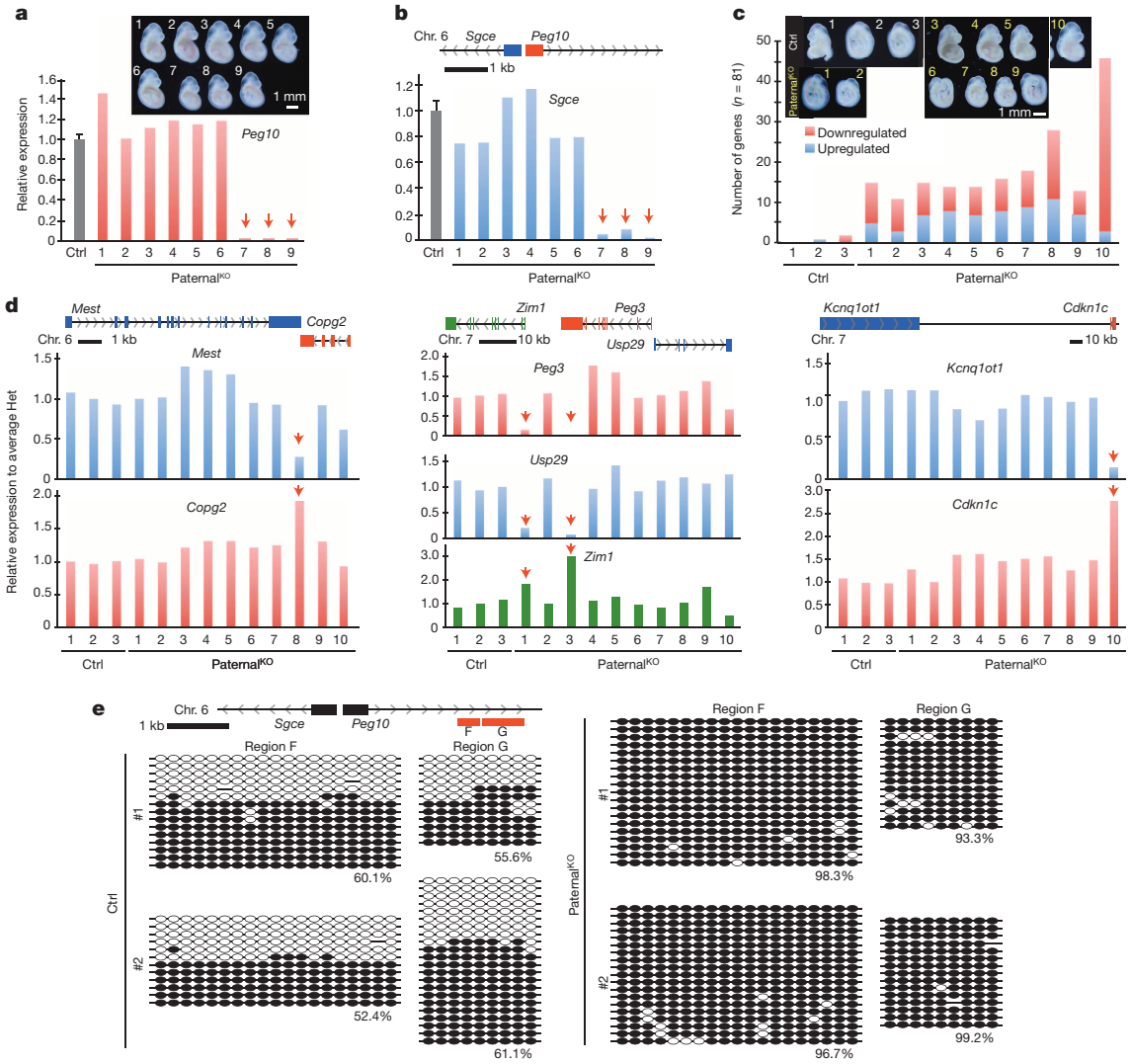

Figure 3 | *Tet1* paternal knockout embryos and placentae exhibit imprinting defects. **a**, **b**, qRT–PCR analysis of *Peg10* (**a**) and *Sgce* (**b**) of E9.5 embryos from a single litter. The pup number corresponds to that in the inserted image in panel **a**. Arrows indicate the samples showing marked reduction in *Peg10* and *Sgce* expression. The average value of control embryos ($n = 13$) is set as 1. Error bars indicate s.e.m. The genomic location of *Peg10* and *Sgce* genes is indicated at the top of panel **b**. **c**, Number of up- and downregulated imprinted genes in each of the paternal^{KO} embryos compared to the average FPKM (fragments per kilobase of exon per million fragments mapped) value of control embryos analysed by RNA-seq (cutoff FC >1.5). A total of 81 autosomal imprinted genes expressed in embryos (FPKM >0.4) was used in this analysis. The pup number corresponds to the inserted images. **d**, Relative expression level of imprinted genes at E9.5 embryos analysed by RNA-seq. Arrows indicate the samples showing marked changes in expression levels. The average FPKM value of three control embryos is set as 1. The genomic locations of each gene are indicated at the top of the diagrams. The pup number corresponds to the inserted images in panel **c**. **e**, Bisulphite sequencing analysis of *Peg10* DMR of E9.5 embryos. The analysed region is indicated at the top of the diagram. Each CpG is represented by a circle with methylation and non-methylation represented by open and filled circles, respectively. The percentages of DNA methylation are indicated.

the sites already exhibited increased DNA methylation in E13.5 male PGCs, and 90 of them exhibited a more than 10% increase (Fig. 4c, Extended Data Fig. 5c and Supplementary Table 7). Notably, a number of imprinted gene loci, including 7 out of 12 commonly covered known germline DMRs, were significantly enriched among these common hypermethylated sites (Fig. 4d, Extended Data Figs 6 and 7, and Supplementary Table 8). This indicates that most of the hypermethylation in the paternal^{KO} embryos can be traced back to sperm and E13.5 PGCs, and clearly demonstrates that hypermethylation in *Tet1* knockout sperm is mainly caused by defective PGC reprogramming. Notably, hypermethylation of meiotic genes was only observed in PGCs, not in sperm (Extended Data Fig. 6a, c). This indicates that passive demethylation and/or other Tet proteins may compensate for the Tet1 deficiency during spermatogenesis, which may explain why the meiotic phenotype is only observed in *Tet1*-null females[7]. Consistent with the Tet1 expression dynamics in PGCs and its capacity to oxidize 5mC to 5hmC, temporal enrichment of 5hmC in DMRs of *Kcnq1ot1*, *Peg3*, *Peg10* and *Igf2r* has been previously reported in reprogramming PGCs[11]. The 5hmC in PGCs generated by Tet1 has probably been diluted via a replication-dependent manner[12,13].

To understand why only a limited number of sites were hypermethylated in response to Tet1 depletion, we analysed the methylation dynamics of these hypermethylated sites during PGC reprogramming. Previous studies have established that PGC demethylation takes place in two stages[14]. The first wave of demethylation completes before E9.5 as more than 70% of CpGs have already been demethylated in E9.5 PGCs. Consistently, most of the RRBS-covered sites have already been demethylated at the early phase of control PGCs, as the average methylation level in E9.5 PGCs dropped to 6.4% (Fig. 4e). Because Tet1 is not upregulated until after E9.5, the first wave of demethylation is Tet1-independent[7,12]. In contrast, Tet1-affected sites remain to be methylated even in E10.5 and E11.5 PGCs, indicating that Tet1 targets are enriched in the

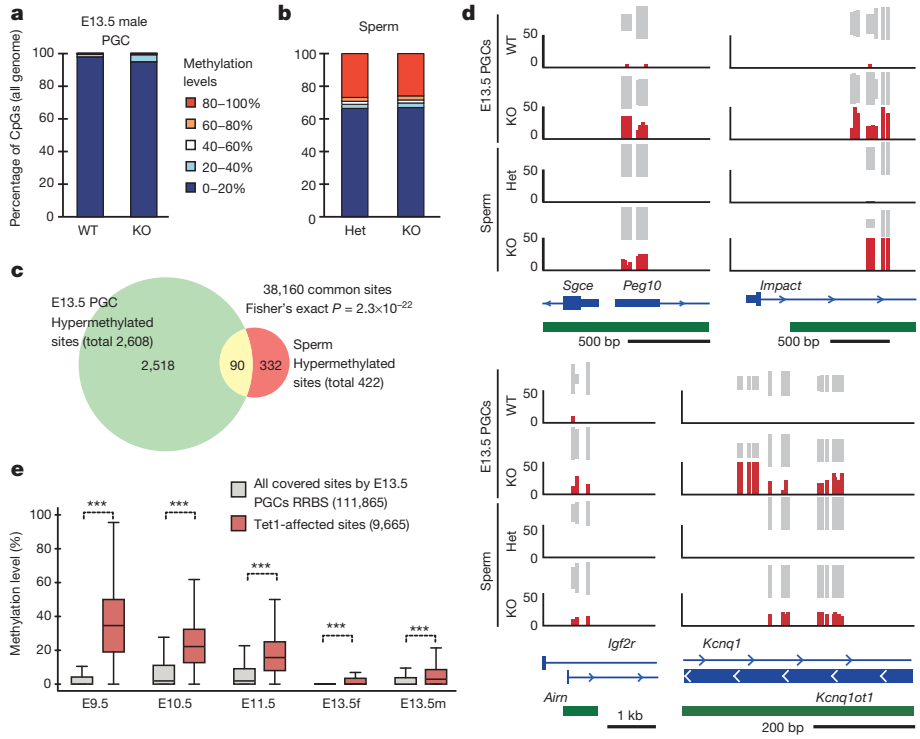

Figure 4 | Locus-specific hypermethylation in *Tet1* knockout PGCs and sperm. **a**, **b**, Genome methylation state of E13.5 PGCs (**a**) and sperm (**b**). **c**, Venn diagram showing the overlap between hypermethylated sites (increased >10%) in *Tet1* knockout PGCs and sperm. **d**, Representative DNA methylation profiles of imprinted genes in E13.5 male PGCs and sperm analysed by RRBS. Vertical grey lines represent the sequence read depth for each cytosine scored, and 30 reads are shown at the most. The vertical red lines represent percentage of methylation for each cytosine scored, which range from 0% to 50%. For each gene, RefSeq exon organization (blue) and location of CGIs (green) are shown at the bottom. **e**, Methylation dynamics of Tet1-affected sites. Methylation level of hypermethylated sites in *Tet1* knockout E13.5 PGCs are analysed based on published data sets[14]. Note that methylation levels of Tet1-affected sites are significantly higher in E9.5 to E11.5 compared to all covered sites. Middle line in the coloured space indicates the median, edges the 25th/75th percentiles, and whiskers the 2.5th/97.5th percentiles. $***P < 1.0 \times 10^{-15}$.

late-demethylated group[14,15] (Fig. 4e and Extended Data Fig. 8a). Indeed, more than 40% of late-demethylated promoters identified previously[14] exhibited hypermethylation in *Tet1* knockout PGCs ($P < 1.0 \times 10^{-15}$, Extended Data Fig. 8b). These data indicate that Tet1 has a major role in the second wave of demethylation in PGCs. Given that these late-demethylated regions affected by Tet1 do not have a consensus DNA sequence motif (data not shown), we believe that instead of being specifically targeted, Tet1 functions to remove the remaining methylation that escaped the first wave of demethylation, including imprinted genes. How the 'late-demethylated regions' are protected from the first wave of DNA demethylation remains to be determined.

During the preparation of this manuscript, one study (ref. 16) reported that some progenies from $Tet1^{-/-}Tet2^{-/-}$ double knockout males crossed with wild-type or $Tet1^{+/-}Tet2^{+/-}$ double-heterozygous females exhibited hypermethylation and dysregulation in a few imprinted genes[16]. To confirm the role of Tet1 in imprinting erasure further, we used the same *Tet1* knockout strain used by ref. 17 and demonstrated similar paternal^{KO} defects (Extended Data Fig. 9), indicating that Tet2 cannot compensate for Tet1's function in imprinting erasure (Supplementary Discussion).

We next asked whether Tet1 also has a role in imprinting erasure in the female germ line. To this end, we generated Tet1 maternal knockout (maternal^{KO}) mice by crossing *Tet1* knockout females with wild-type males. We observed lethality in about 25% of maternal^{KO} embryos with relatively normal placenta (Extended Data Fig. 10a, b). The placentae of the survived embryos were significantly larger compared to that of the control although they had a comparable body size (Extended Data Fig. 10c, d). qRT–PCR analysis revealed silencing of paternally imprinted genes such as *Meg3/Dlk1* and *Mirg* in all of the placentae of dead embryos (Extended Data Fig. 10e). Additionally, *Rasgrf1* was also upregulated in some of the maternal^{KO} placentae (for example, numbers 6, 10 and 11). Consistent with abnormal expression of *Meg3/Dlk1*, *Mirg* and *Rasgrf1*, hypermethylation of both intergenic (IG)-DMR and *Rasgrf1* was observed in abnormal placentae (Extended Data Fig. 10f, g). These results indicate that Tet1 is involved in imprinting erasure of not only maternal DMRs in the male germ line, but also paternal DMRs in the female germ line.

Collectively, our studies clearly demonstrate that Tet1 has an important role in the erasure of genomic imprinting. Although some factors, such as *Aid* and *Tdg*, have been proposed to have a role in imprinting erasure, evidence demonstrating a loss of functional effect at the next generation is still missing[18,19]. As far as we know, our current study is the first that reports a factor critical for imprinting erasure with physiological evidence. Consistent with our study, another study (ref. 20) also revealed that Tet1-mediated oxidation is essential for the erasure of genomic imprinting in cell fusion experiments[20]. The phenotypic variation observed in each *Tet1* paternal^{KO} embryo can be explained by the variable DMR methylation remaining in each *Tet1* knockout sperm (Extended Data Fig. 11 and Supplementary Discussion). It is well known that abnormalities in genomic imprinting can cause various human diseases[1]. The conservation of Tet1 function in humans and mice raises the possibility that human Tet1 may also have an important role in imprinting erasure (Supplementary Discussion). Future studies should reveal whether dysfunction of Tet1 contributes to growth restriction or other imprinting-related syndromes.

METHODS SUMMARY

Animals. *Tet1* gene-trap mice were generated as previously described[7]. *Tet1* paternal^{KO} and control mice were generated by mating littermate males of Tet1-homozygotes or Tet1-heterozygotes with C57BL/6J females.

qRT–PCR and RNA-seq. For expression analysis, cDNAs were synthesized from total RNA by using Superscript III First-Strand synthesis (Invitrogen) with random

primer sets. Quantitative PCR (qPCR) reactions were performed with gene-specific primer sets (Supplementary Table 9). Relative expression levels were calculated on the basis of comparative Ct values after normalizing with *Gapdh*. For RNA-seq, the libraries prepared from purified mRNA were sequenced on an Illumina HISEQ 2500. RNA-seq data analysis was performed with Tophat and Cufflinks using the UCSC mm9 annotation.

Bisulphite sequencing and RRBS. BS-seq was performed using the EZ DNA methylation Gold kit (Zymo Research) following the manufacturer's instructions. Primers for BS-seq are listed in Supplementary Table 9 (refs 21, 22). For RRBS, the libraries were generated from MspI-digested genomic DNA and sequenced on an Illumina Hiseq 2500 as previously described, with some modifications[23]. All obtained reads were trimmed and mapped against the mouse genome (mm9 build) with Bismark v0.7.12, and the methylation call for every single CpG was extracted by bismark methylation extractor script. The CpGs covered by at least 8 reads were analysed. On the basis of the assumption that there should not be any hypomethylated sites in *Tet1* knockout PGCs, the estimated empirical false discovery rate (FDR) of hypomethylated sites in *Tet1* knockout PGCs at a 10% methylation change cutoff is 0.054. At a 20% methylation change cutoff, the FDR is 0.032.

Online Content Any additional Methods, Extended Data display items and Source Data are available in the online version of the paper; references unique to these sections appear only in the online paper.

Received 28 May; accepted 31 October 2013.
Published online 1 December 2013.

1. Bartolomei, M. S. & Ferguson-Smith, A. C. Mammalian genomic imprinting. *Cold Spring Harb. Perspect. Biol.* **3,** a002592 (2011).
2. Li, Y. & Sasaki, H. Genomic imprinting in mammals: its life cycle, molecular mechanisms and reprogramming. *Cell Res.* **21,** 466–473 (2011).
3. Kaneda, M. *et al.* Essential role for *de novo* DNA methyltransferase Dnmt3a in paternal and maternal imprinting. *Nature* **429,** 900–903 (2004).
4. Ito, S. *et al.* Role of Tet proteins in 5mC to 5hmC conversion, ES-cell self-renewal and inner cell mass specification. *Nature* **466,** 1129–1133 (2010).
5. Tahiliani, M. *et al.* Conversion of 5-methylcytosine to 5-hydroxymethylcytosine in mammalian DNA by MLL partner TET1. *Science* **324,** 930–935 (2009).
6. Shen, L. & Zhang, Y. 5-Hydroxymethylcytosine: generation, fate, and genomic distribution. *Curr. Opin. Cell Biol.* **25,** 289–296 (2013).
7. Yamaguchi, S. *et al.* Tet1 controls meiosis by regulating meiotic gene expression. *Nature* **492,** 443–447 (2012).
8. Nelissen, E. C. M., van Montfoort, A. P. A., Dumoulin, J. C. M. & Evers, J. L. H. Epigenetics and the placenta. *Hum. Reprod. Update* **17,** 397–417 (2011).
9. Ono, R. *et al.* Deletion of *Peg10*, an imprinted gene acquired from a retrotransposon, causes early embryonic lethality. *Nature Genet.* **38,** 101–106 (2006).
10. Ono, R. *et al.* Identification of a large novel imprinted gene cluster on mouse proximal chromosome 6. *Genome Res.* **13,** 1696–1705 (2003).
11. Hackett, J. A. *et al.* Germline DNA demethylation dynamics and imprint erasure through 5-hydroxymethylcytosine. *Science* **339,** 448–452 (2013).
12. Kagiwada, S., Kurimoto, K., Hirota, T., Yamaji, M. & Saitou, M. Replication-coupled passive DNA demethylation for the erasure of genome imprints in mice. *EMBO J.* **32,** 340–353 (2013).
13. Yamaguchi, S. *et al.* Dynamics of 5-methylcytosine and 5-hydroxymethylcytosine during germ cell reprogramming. *Cell Res.* **23,** 329–339 (2013).
14. Seisenberger, S. *et al.* The dynamics of genome-wide DNA methylation reprogramming in mouse primordial germ cells. *Mol. Cell* **48,** 849–862 (2012).
15. Kobayashi, H. *et al.* High-resolution DNA methylome analysis of primordial germ cells identifies gender-specific reprogramming in mice. *Genome Res.* **23,** 616–662 (2013).
16. Dawlaty, M. M. *et al.* Combined deficiency of Tet1 and Tet2 causes epigenetic abnormalities but is compatible with postnatal development. *Dev. Cell* **24,** 310–323 (2013).
17. Dawlaty, M. M. *et al.* Tet1 is dispensable for maintaining pluripotency and its loss is compatible with embryonic and postnatal development. *Cell Stem Cell* **9,** 166–175 (2011).
18. Cortellino, S. *et al.* Thymine DNA glycosylase is essential for active DNA demethylation by linked deamination-base excision repair. *Cell* **146,** 67–79 (2011).
19. Popp, C. *et al.* Genome-wide erasure of DNA methylation in mouse primordial germ cells is affected by AID deficiency. *Nature* **463,** 1101–1105 (2010).
20. Piccolo, F. M. *et al.* Different roles for Tet1 and Tet2 proteins in reprogramming-mediated erasure of imprints induced by EGC fusion. *Mol. Cell* **49,** 1023–1033 (2013).
21. Kobayashi, H. *et al.* Bisulfite sequencing and dinucleotide content analysis of 15 imprinted mouse differentially methylated regions (DMRs): paternally methylated DMRs contain less CpGs than maternally methylated DMRs. *Cytogenet. Genome Res.* **113,** 130–137 (2006).
22. Tomizawa, S.-i. *et al.* Dynamic stage-specific changes in imprinted differentially methylated regions during early mammalian development and prevalence of non-CpG methylation in oocytes. *Development* **138,** 811–820 (2011).
23. Gu, H. *et al.* Preparation of reduced representation bisulfite sequencing libraries for genome-scale DNA methylation profiling. *Nature Protocols* **6,** 468–481 (2011).

Supplementary Information is available in the online version of the paper.

Acknowledgements We thank W. Jiang for help with FACS sorting of PGCs; A. Inoue, S. Matoba and D. Cai for critical reading of the manuscript. This project is supported by NIH U01DK089565 (to Y.Z.). S.Y. is supported by a postdoctoral fellowship from the Japan Society for the Promotion of Science (JSPS). Y.Z. is an investigator of the Howard Hughes Medical Institute.

Author Contributions S.Y. and Y.Z. conceived the project, designed the experiments and wrote the manuscript; S.Y., L.S., Y.L. and D.S. performed experiments and analysed the data.

Author Information The accession number for the RNA-seq and RRBS data presented in this study is available from the Gene Expression Omnibus (GEO) database under accession GSE49764. Reprints and permissions information is available at www.nature.com/reprints. The authors declare no competing financial interests. Readers are welcome to comment on the online version of the paper. Correspondence and requests for materials should be addressed to Y.Z. (yzhang@genetics.med.harvard.edu).

METHODS

Mice. All animal studies were performed in accordance with guidelines of the Institutional Animal Care and Use Committee at Harvard Medical School. The *Tet1* knockout mouse strain (B6;129S4-Tet1$^{tm1.1Jae}$/J) was purchased from Jackson Laboratory[17]. All male mice were mated with C57BL/6J female and the mating is timed in the way that appearance of vaginal plug at noon is defined as embryonic day (E) 0.5. E19.5 embryos and placentae were collected by dissecting pregnant females with progesterone injection at E17.5 and E18.5. All data presented were generated by using three or four separate mating pairs as biological replicates.

Histology. Embryos and placentae in the uterus were fixed in 4% paraformaldehyde, dehydrated in ethanol, and embedded in paraffin. For histological analysis, sections (5 μm) were stained with haematoxylin and eosin.

RNA isolation and qRT–PCR. Dissected embryos and placentae were homogenized with a pestle. Total RNAs were isolated with TRizol (Life technologies), and cDNAs were generated with random primer sets and Superscript III first-strand synthesis system (Invitrogen). Real-time qPCR reactions were performed on an ABI ViiA7 sequence detection system (Applied Biosystems) using SYBR green (Applied Biosystems). Relative gene expression levels were calculated using comparative Ct values, in which Ct is the cycle threshold number, and normalized to *Gapdh*. qRT–PCR primers are listed in Supplementary Table 9.

PGC purification for RRBS. E13.5 male PGCs were purified as described previously[7]. Briefly, the transgenic mouse line containing the GOF18DPE-EGFP [Tg(Pou5f1-EGFP)] transgene was purchased from Jackson Laboratory. E13.5 genital ridge cells were dissociated with 0.05% trypsin/EDTA treatment with pipetting. After washing with phosphate buffer medium (PB1)/BSA solution, tissues were incubated in hyaluronidase, washed and then re-suspended in PBS. Germ cells were purified based on the expression of GFP using FACS Aria II flow cytometry (BD Bioscience), and stored in −80 °C until use. Two biological replicates for *Tet1* knockout and wild-type PGCs were combined and split into two as the technical replicates.

RNA-seq library preparation and data analysis. Total RNA was purified with an RNeasy Mini kit (Qiagen), in which an on-column DNase treatment was included. 500 ng of purified RNA was then subjected to mRNA isolation and library preparation using a NEBNext Ultra RNA Directional Library Prep kit for Illumina with the Poly(A) mRNA Magnetic Isolation Module (NEB) following manufacturer's instructions. Libraries were pooled and sequenced on an Illumina HISEQ 2500 (single-end, 50 bp). RNA-seq data analysis was performed with Tophat and Cufflinks using the UCSC mm9 annotation[24]. Functional annotation of the dysregulated genes was performed with DAVID[25].

Bisulphite sequencing and RRBS. BS-seq was performed using the EZ DNA methylation Gold kit (Zymo Research) following the manufacturer's instruction. Primers for BS-seq are listed in Supplementary Table 9 (refs 21, 22). For RRBS, the libraries were generated essentially as previously described[23,26], with some modifications. Briefly, DNA was digested with MspI (NEB), and then subjected to end repair, and ligation of methylated custom adaptors (forward 5′-ACACTCTTTCCCTACACGACGCTCTTCCGATC*T-3′; reverse 5′-/5Phos/GATCGGAAGAGCACACGTCTGAACTCCAGTC-3′, where the asterisk indicates phosphorothioate bond) with a NEBNext Ultra DNA Library Prep kit from Illumina (NEB). Size selection was conducted by purifying the adaptor-ligated DNA twice with 1.5× SPRIselect beads (Beckman Coulter). Size-selected libraries were treated with sodium bisulphite using the EpiTect Fast Bisulphite Conversion kit (Qiagen). After clean-up, the optimal, minimum PCR cycle numbers required to generate the final libraries were determined by qPCR using KAPA 2G Robust HotStart ReadyMix (KAPA) with 0.3× SYBR I. Final libraries were generated by scaled-up PCR reactions (without SYBR I) using the cycles determined above with barcoded primers from the NEBNext Multiplex Oligos kit (NEB), and purified with 1.2× SPRIselect beads. Libraries were pooled and sequenced on an Illumina Hiseq 2500 (single-end, 50 bp).

Adaptor trimming for raw reads from each sample was performed using Trim Galore (Babraham Bioinformatics), and the data quality was examined using FastQC (Babraham Bioinformatics). The trimmed reads were mapped against the mouse genome (mm9 build) with Bismark v0.7.12 (ref. 27), and the methylation call for every single C was extracted by bismark methylation extractor script. All programs were performed with default setting. We only keep the CpGs that were covered by at least 8 reads (common 8x CpGs). The methylation pattern was visualized by Integrative Genomics Viewer (IGV)[7]. For 100-bp tiles and the promoters, reads for the CpGs that were covered at least eight times in each sample were pooled and used to estimate the methylation level by taking the number of reads reporting a C, divided by the total number of reads reporting a C or T. We kept the 100-bp sites and the promoters with at least 2 and 4 common 8× CpGs for subsequent analyses. Repetitive regions were masked before DMR calling. More than 10% methylation level changes were required to be classified as changed sites or promoters. On the basis of the assumption that no hypomethylated sites in *Tet1* knockout PGCs should appear, estimated empirical false discovery rate (FDR) by the number of hypomethylated sites in *Tet1* knockout PGCs was 0.054. At a 20% methylation change cutoff, the FDR is 0.032. Annotation of CpG islands was obtained from a previous report based on pull-down experiments[28]. Promoters were defined as the region −1.5 kb to +1.5 kb of the transcription start site as annotated in Refseq genes. Repeat annotations were extracted from the UCSC Table Browser Repeat-Masker track (mm9 build). DMRs were functionally characterized by GREAT[29] using the Mouse Genome Informatics (MGI) Phenotype ontology[30]. Publically available data sets for whole-genome bisulphite sequencing (WGBS) data sets in PGCs[14,15] were included in this analysis where indicated. For WGBS data analyses, all the informative CpGs were used, and the methylation level in a region was estimated by taking the number of reads reporting a C, divided by the total number of reads reporting a C or T. We required that there were at least 20 methylated or unmethylated cytosine observations in the region for each sample.

24. Trapnell, C. *et al.* Differential gene and transcript expression analysis of RNA-seq experiments with TopHat and Cufflinks. *Nature Protocols* **7,** 562–578 (2012).
25. Huang, D. W., Sherman, B. T. & Lempicki, R. A. Systematic and integrative analysis of large gene lists using DAVID bioinformatics resources. *Nature Protocols* **4,** 44–57 (2009).
26. Boyle, P. *et al.* Gel-free multiplexed reduced representation bisulfite sequencing for large-scale DNA methylation profiling. *Genome Biol.* **13,** R92 (2012).
27. Krueger, F. & Andrews, S. R. Bismark: a flexible aligner and methylation caller for Bisulfite-Seq applications. *Bioinformatics* **27,** 1571–1572 (2011).
28. Illingworth, R. S. *et al.* Orphan CpG islands identify numerous conserved promoters in the mammalian genome. *PLoS Genet.* **6,** e1001134 (2010).
29. McLean, C. Y. *et al.* GREAT improves functional interpretation of cis-regulatory regions. *Nature Biotechnol.* **28,** 495–501 (2010).
30. Blake, J. A. *et al.* The mouse genome database genotypes:phenotypes. *Nucleic Acids Res.* **37,** D712–D719 (2009).

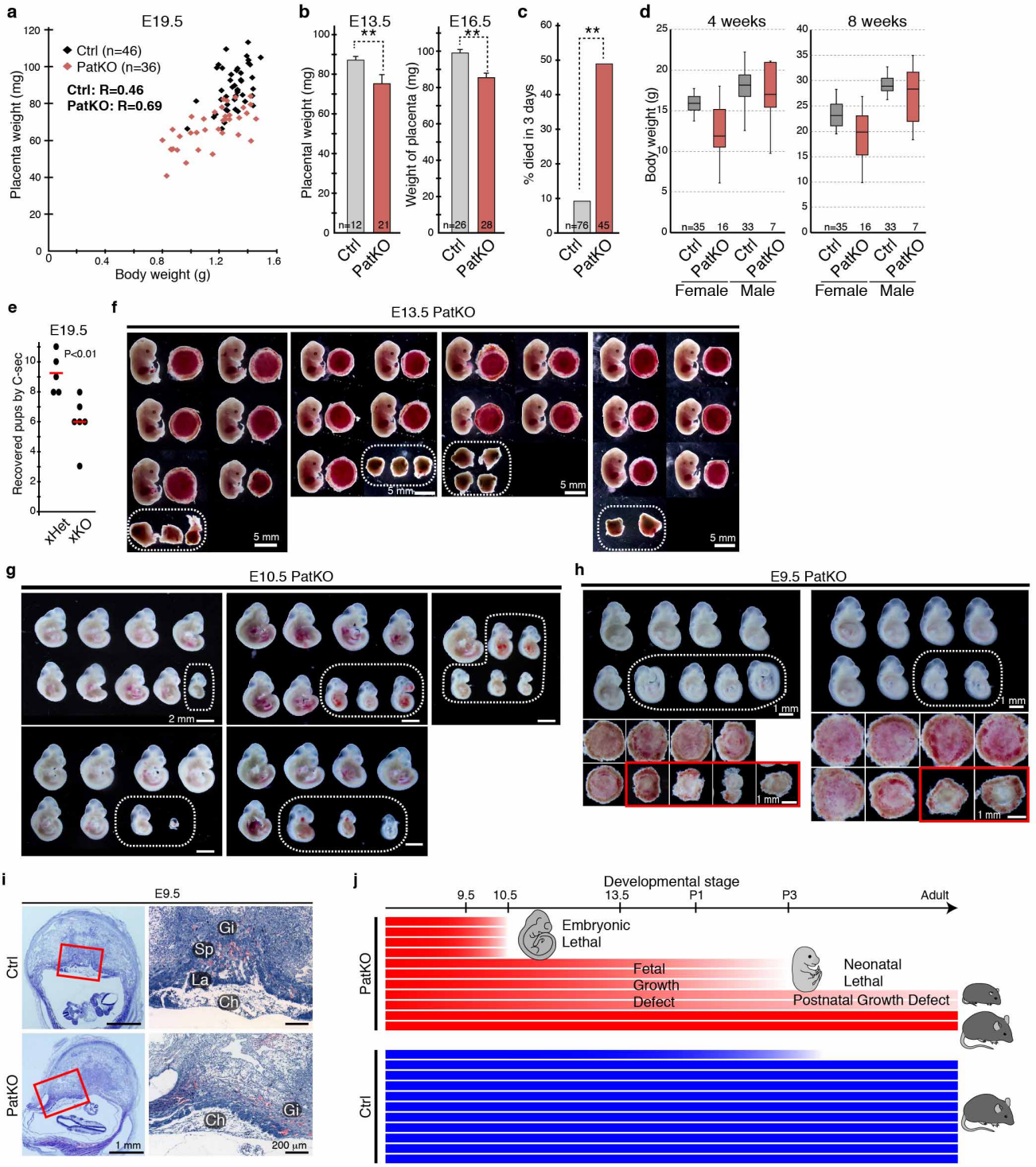

Extended Data Figure 1 | *Tet1* paternal knockout mice exhibit various phenotypes, including fetal and postnatal growth defects, and neonatal and embryonic lethality. **a**, Scatter plot of body and placental sizes for each pup. **b**, Average placental weight of E13.5 and E16.5 embryos. Error bars indicate s.e.m. $^{**}P < 0.01$. **c**, Percentage of pups that die within 3 days of birth. $^{**}P < 0.01$. **d**, Box plot presentation of body weights of 4- and 8-week-old control and paternal^{KO} mice. Note that paternal^{KO} mice exhibited a larger variation and smaller body weight compared to the control mice. Middle lines in the coloured boxes indicate the median, box edges indicate the 25th/75th percentiles, and whiskers the 0th/100th percentiles. **e**, Mating scores of *Tet1*$^{+/-}$ male × wild-type female (×Het) and *Tet1*$^{-/-}$ male × wild-type female (×KO) mice. Black dots indicate the numbers of pups for each litter recovered by Caesarean section at E19.5. Red lines indicate the mean litter size. **f**, The embryos and placentae at E13.5 recovered from four litters of *Tet1* paternal^{KO} mice. The dotted ovals indicate the residues of absorbed embryos. **g**, E10.5 paternal^{KO} embryos recovered from five litters. Dotted oval indicates morphologically abnormal embryos. **h**, Top: E9.5 paternal^{KO} embryos recovered from two litters. Dotted ovals indicate small embryos whose placentae are morphologically abnormal. Bottom: placentae corresponding to the embryos on the top panels. Red rectangles indicate morphologically abnormal placentae. **i**, Representative images of haematoxylin and eosin staining of E9.5 placentae. Red rectangles indicate the enlarged regions shown at the right panels. Ch, chorionic plate; Gi, trophoblast giant cells; La, labyrinthine zone; Sp, spongioblast. **j**, Schematic representation of *Tet1* paternal^{KO} phenotypes. Each bar represents an individual mouse. About 40% of paternal^{KO} mice exhibit early embryonic lethality. About half of the remaining mice die neonatally, and about half of the surviving mice show postnatal growth defects. In contrast, abnormality is rarely observed in control, except at the neonatal stage (less than 10%).

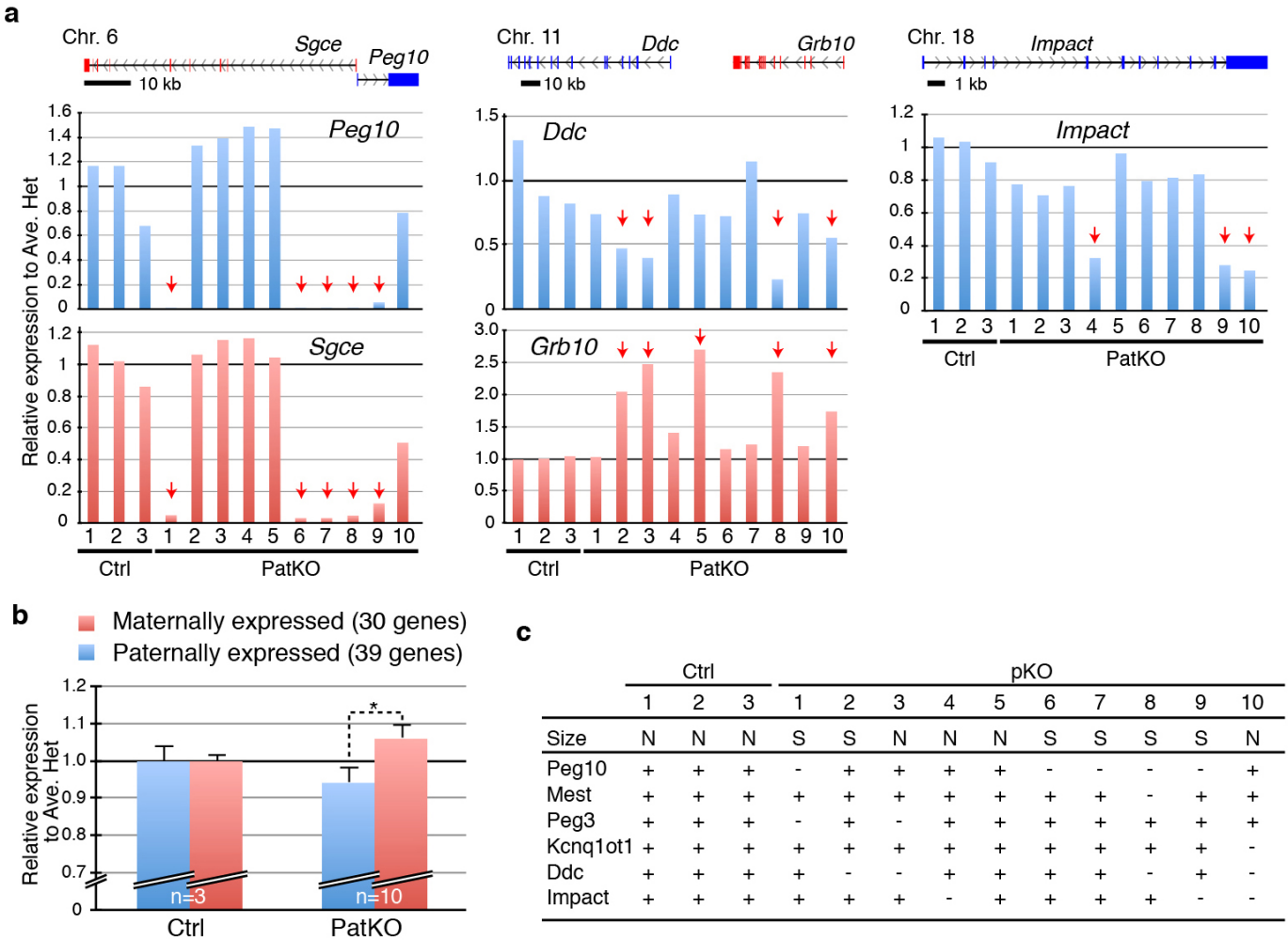

	Ctrl			pKO									
	1	2	3	1	2	3	4	5	6	7	8	9	10
Size	N	N	N	S	S	N	N	N	S	S	S	S	N
Peg10	+	+	+	-	+	+	+	+	-	-	-	-	+
Mest	+	+	+	+	+	+	+	+	+	+	-	+	+
Peg3	+	+	+	-	+	-	+	+	+	+	+	+	+
Kcnq1ot1	+	+	+	+	+	+	+	+	+	+	+	+	-
Ddc	+	+	+	+	-	-	+	+	+	+	-	+	-
Impact	+	+	+	+	+	+	-	+	+	+	+	-	-

Extended Data Figure 2 | Dysregulation of imprinted genes in *Tet1* paternal knockout embryos. **a**, Relative expression levels of imprinted genes in E9.5 embryos analysed by RNA-seq. The averaged FPKM (fragments per kb of exon per million fragments mapped) value of three control embryos is set as 1. Arrows indicate dysregulated embryos. The location of each gene is indicated in the diagram on top of the panel. **b**, Relative average expression change of maternally and paternally imprinted genes. The imprinted genes that are highly expressed in E9.5 embryos (FPKM >1.0) are used in this analysis. Error bars indicate s.e.m. $*P < 0.05$. **c**, Summary of imprinted genes dysregulated in paternal^{KO} embryos. N, normal size; S, small size; +, normal expression; −, downregulated.

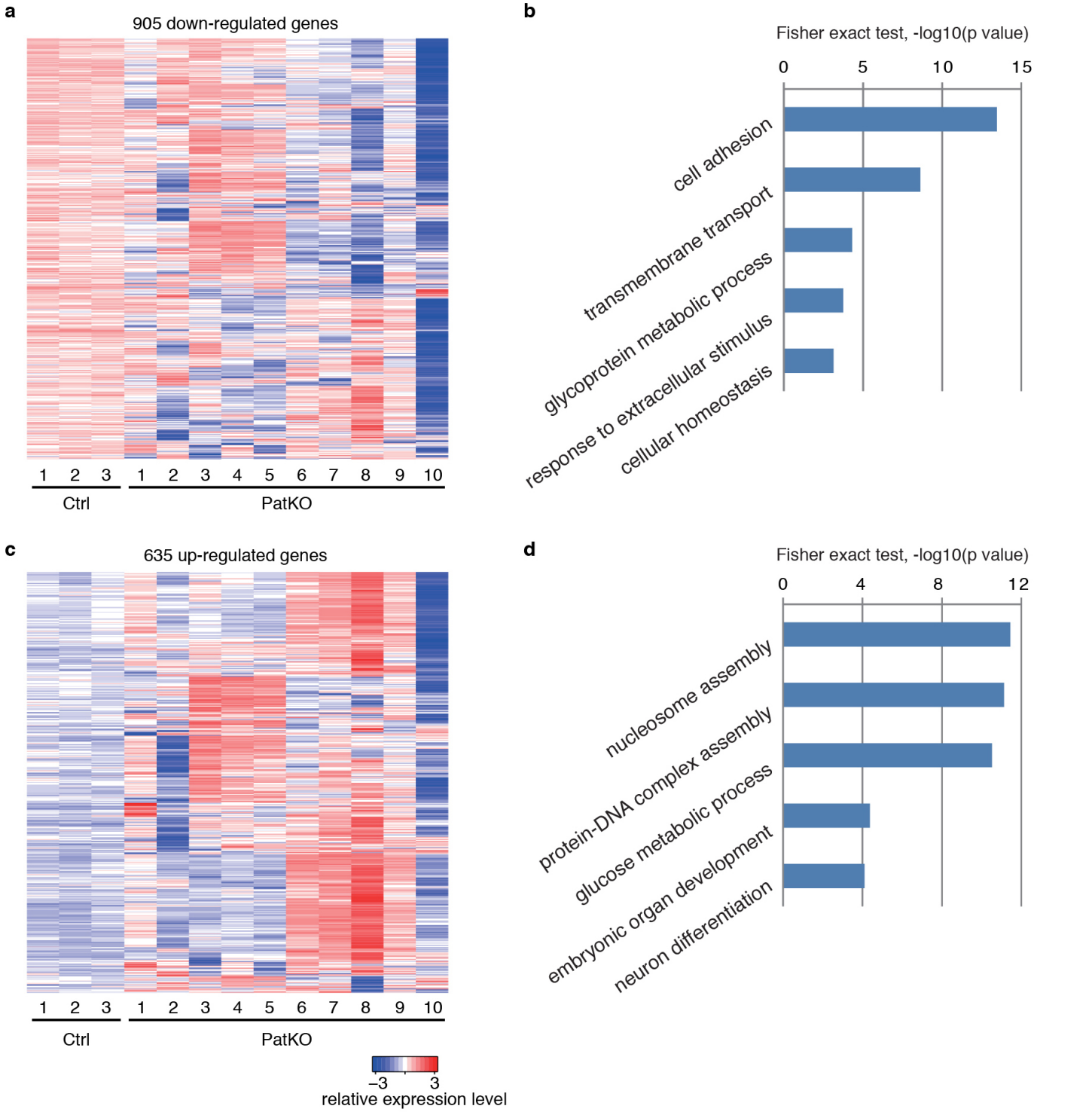

Extended Data Figure 3 | Perturbation of gene expression in *Tet1* paternal knockout embryos. **a**, Heat-map representation of markedly downregulated genes (FC >1.5) in at least two E9.5 paternal^{KO} embryos. Only those genes with significant change in at least two paternal^{KO} embryos were shown. **b**, GO analysis of the 905 downregulated genes. **c**, Heat-map representation of markedly upregulated genes (FC >1.5) in at least E9.5 paternal^{KO} embryos. **d**, GO analysis of the 635 upregulated genes.

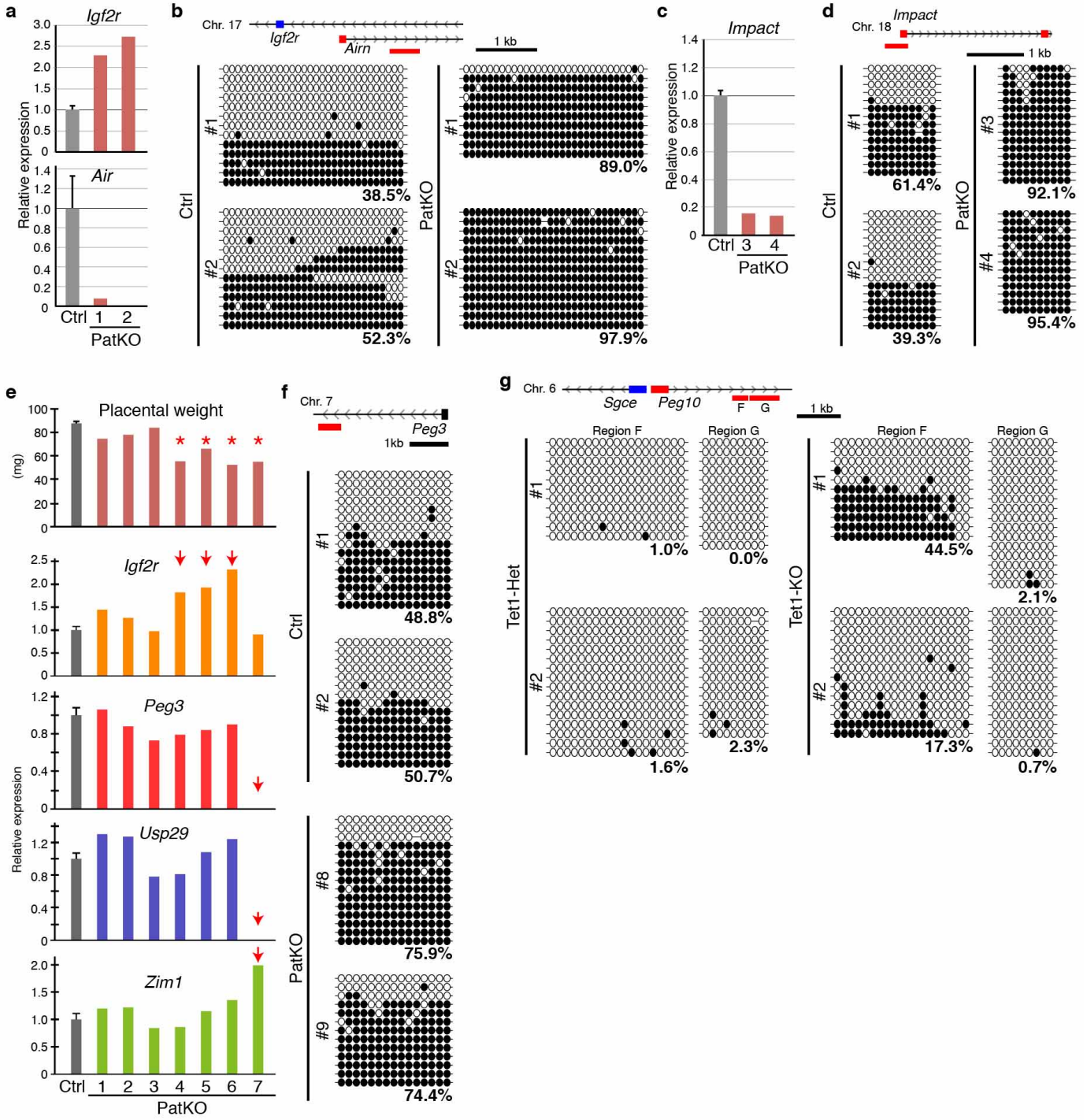

Extended Data Figure 4 | Hypermethylation in germline differentially methylated regions in *Tet1* paternal knockout embryos and placentae, and *Tet1* knockout sperm. **a**, RT–qPCR analysis of *Igf2r* and *Air* in E9.5 embryos. The average value of control embryos ($n = 13$) is set as 1. Error bars indicate s.e.m. **b**, Bisulphite sequencing analysis of *Air–Igf2r* DMR of E9.5 embryos. The analysed region is indicated by a red line at the top of the diagram. Each CpG is represented by a circle with methylation and non-methylation represented by open and filled circles, respectively. The percentages of DNA methylation are indicated. **c**, qRT–PCR analysis of *Impact* in E9.5 embryos. The average value of control embryos ($n = 13$) is set as 1. Error bar indicates s.e.m. **d**, Bisulphite sequencing analysis of *Impact* DMR of E9.5 embryos. The analysed region is indicated by a red line at the top of the diagram. **e**, The weight of individual E19.5 paternal^{KO} placentae (top) and qRT–PCR analysis of several imprinted gene expression patterns in each placenta. The average value of control placentae ($n = 19$) is set as 1. Asterisks indicate small placentae. Arrows indicate the samples showing a marked change in expression levels. Error bars indicate s.e.m. **f**, Bisulphite sequencing analysis of *Peg3* DMR of E19.5 placentae. The analysed region is indicated at the top of the diagram. The percentages of DNA methylation are indicated. **g**, Bisulphite sequencing analysis of the *Peg10* DMR in Tet1-heterozygous and knockout sperm. The analysed region is indicated by a red line at the top of the diagram.

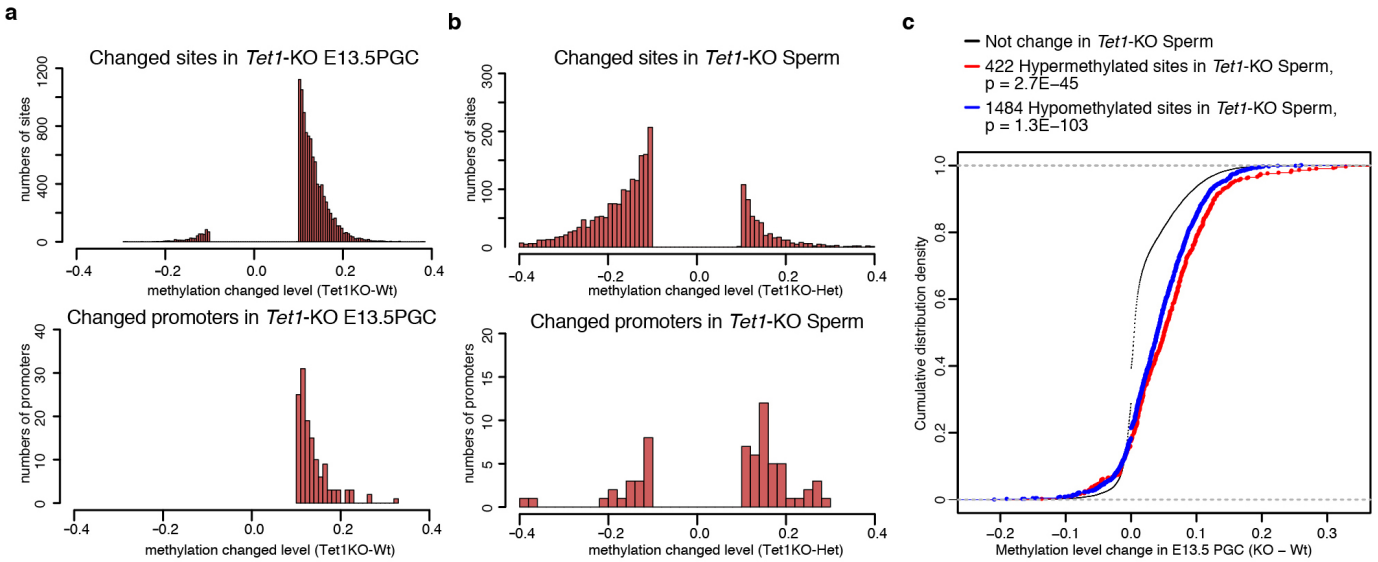

Extended Data Figure 5 | Summary of RRBS analysis. **a**, **b**, Distribution of the level of methylation change for changed sites and promoters in E13.5 PGCs (**a**) and sperm (**b**) (cutoff, 10%). **c**, Cumulative distribution curve of methylation change in E13.5 PGCs for the sites showing methylation change in *Tet1* knockout sperm. Note that methylation levels in E13.5 *Tet1* knockout PGCs of both 422 hypermethylated sites in sperm (red) and 1,484 hypomethylated sites in sperm (blue) are higher than that of non-changed sites.

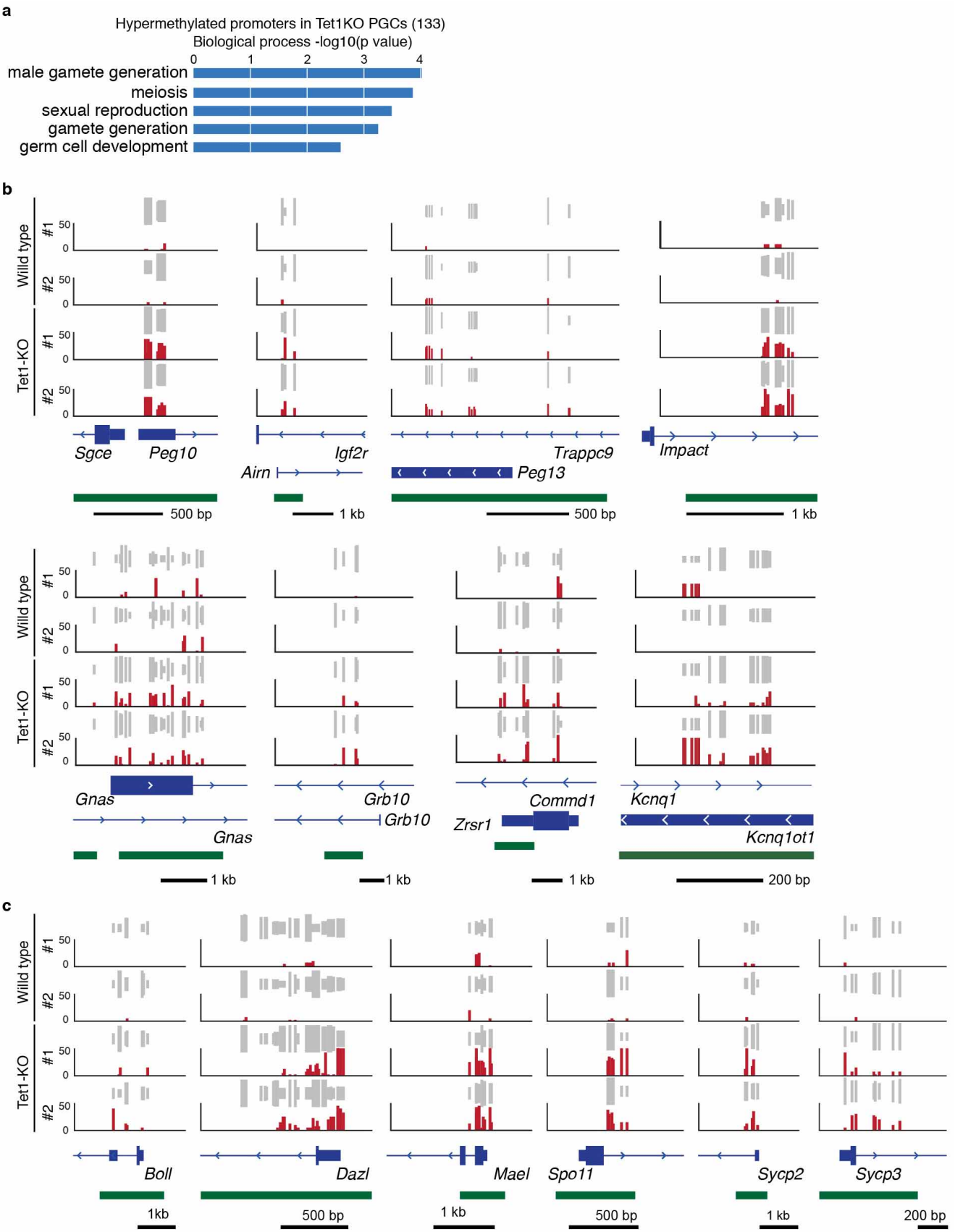

Extended Data Figure 6 | Hypermethylation in *Tet1* knockout E13.5 PGCs at imprinted genes and germline genes. **a**, GO analysis of the genes with hypermethylated promoters in *Tet1* knockout E13.5 PGCs. **b**, **c**, Representative DNA methylation profiles of selected imprinting genes (**b**) and germline genes (**c**) in E13.5 PGCs analysed by RRBS. Vertical grey lines represent the sequence read depth for each cytosine scored, and 30 reads were shown at most. The vertical red lines represent percentage of methylation for each cytosine scored, which range from 0% to 50%. For each gene, RefSeq exon organization (blue) and location of CGIs (green) are shown at the bottom.

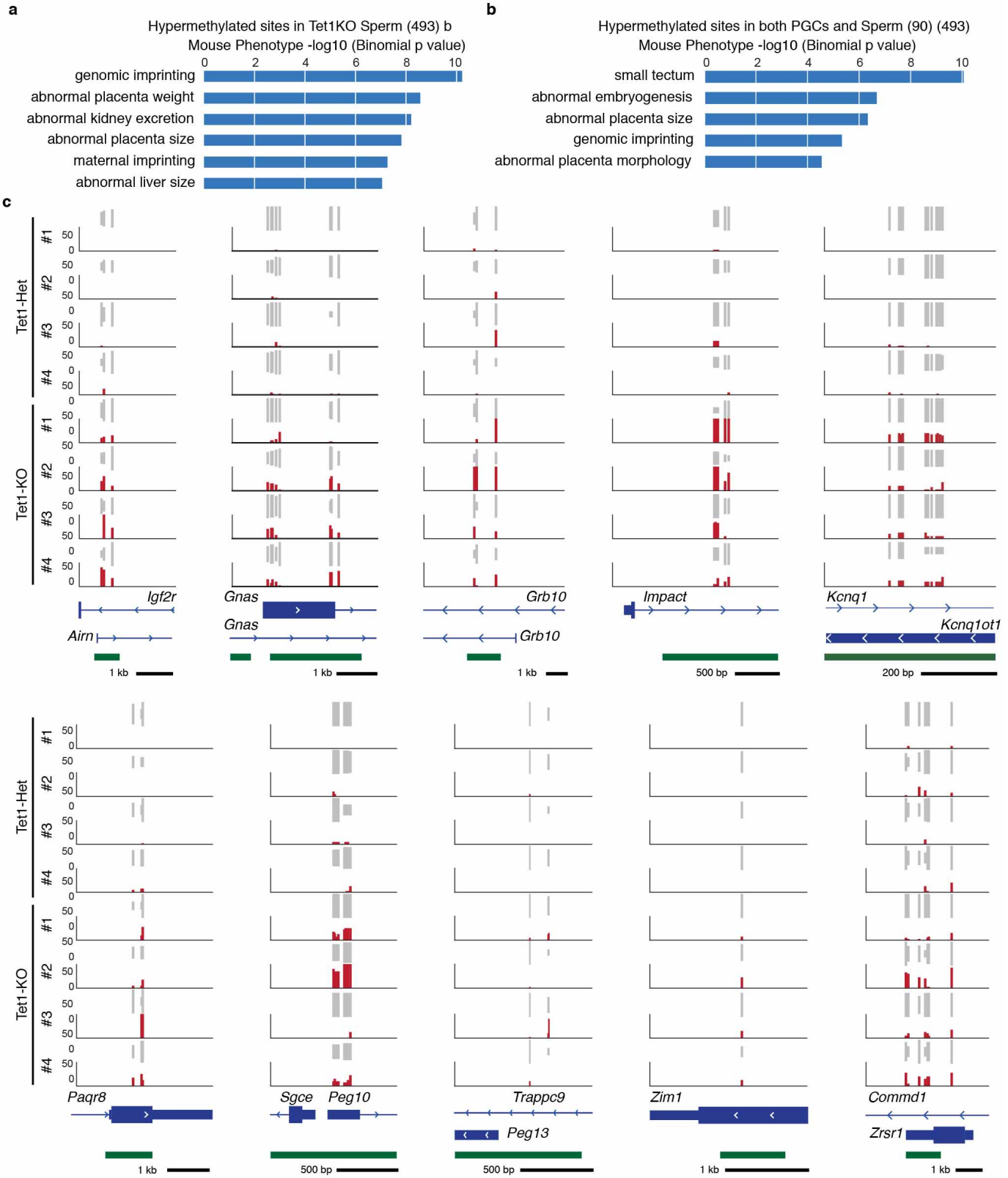

Extended Data Figure 7 | Hypermethylation in *Tet1* knockout sperm at imprinted genes. **a**, **b**, Mouse phenotype ontology enrichment of hypermethylated sites in *Tet1* knockout sperm (**a**) and hypermethylated sites in both *Tet1* knockout E13.5 PGCs and sperm (**b**). **c**, Representative DNA methylation profiles of selected imprinting genes in sperm analysed by RRBS. Vertical grey lines represent the sequence read depth for each cytosine scored, and 30 reads are shown at most. The vertical red lines represent percentage of methylation for each cytosine scored, which range from 0% to 50%. For each gene, RefSeq exon organization (blue) and location of CGIs (green) are shown at the bottom.

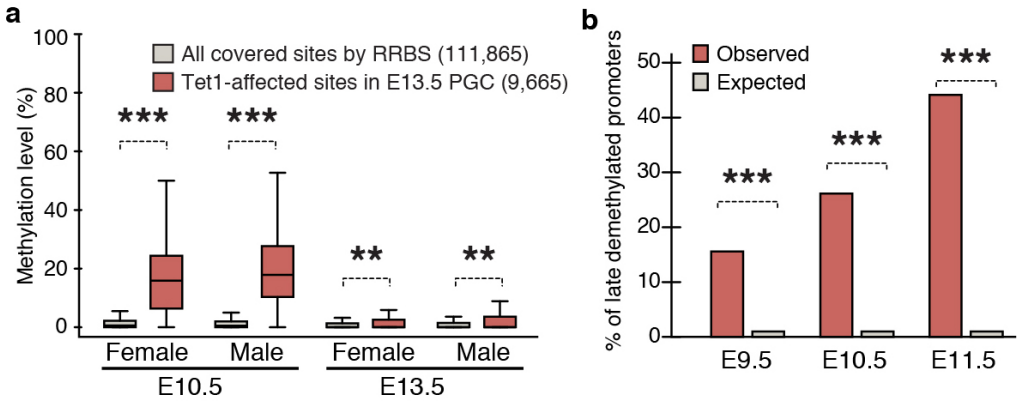

Extended Data Figure 8 | *Tet1* knockout affected loci are enriched in late demethylated regions in PGCs. **a**, Methylation dynamics of the loci that are hypermethylated in *Tet1* knockout E13.5 PGCs. Methylation levels were obtained from a previous study[15]. Middle lines in the coloured boxes indicate the median, box edges indicate the 25th/75th percentiles, and whiskers the 2.5th/97.5th percentiles. **b**, Percentages of hypermethylated promoters in *Tet1* knockout PGCs among late demethylated promoters. The RRBS-covered promoters with >25% methylation in E9.5, E10.5 and E11.5 PGCs (ref. 14) were analysed. ***$P < 1.0 \times 10^{-15}$, **$P < 0.01$.

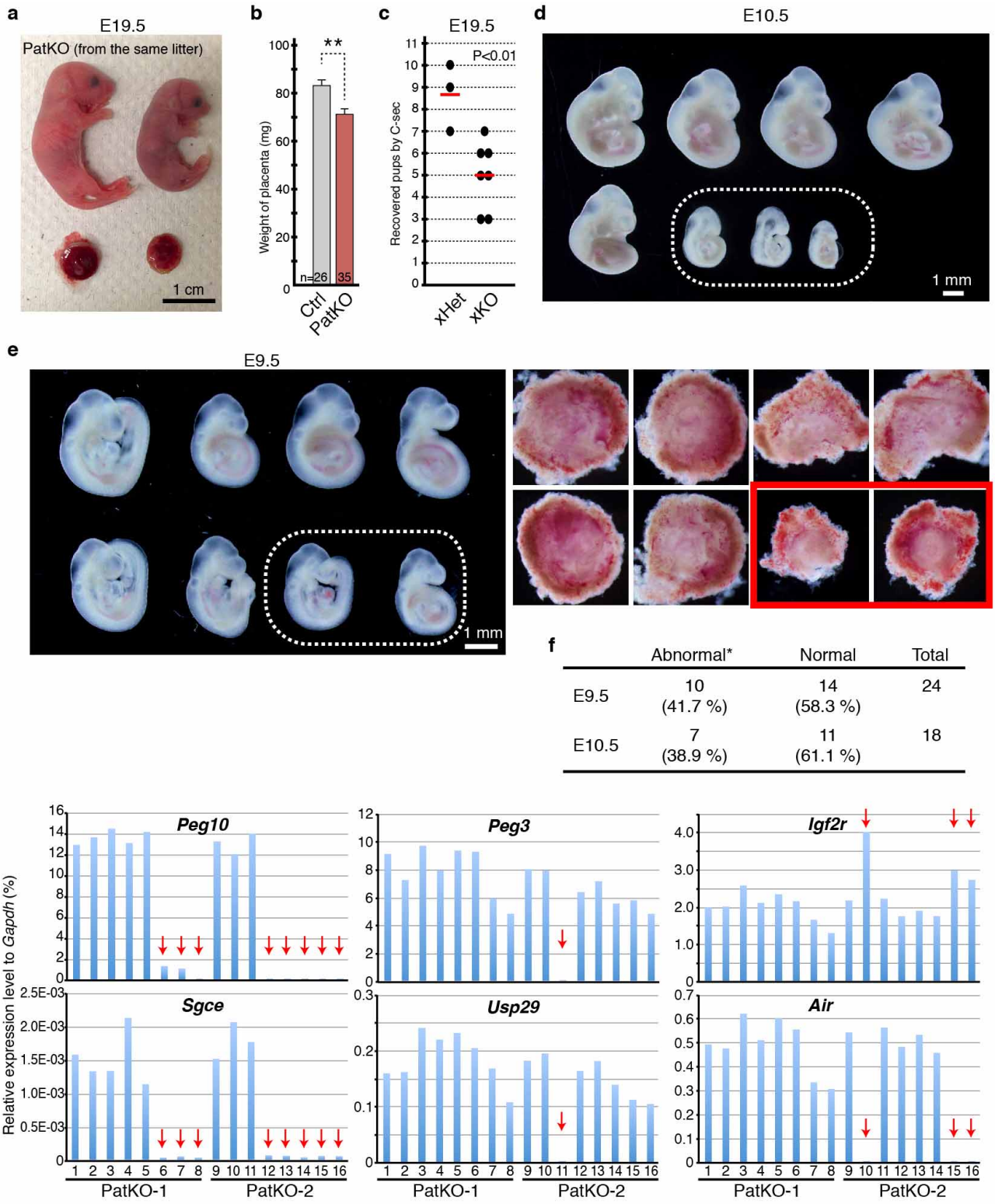

Extended Data Figure 9 | Early embryonic lethality and dysregulation of imprinted gene expression in *Tet1* paternal knockout mice generated by ref. 17. **a**, Representative image of paternal^{KO} pups from the same litter showing big variation in body and placenta sizes. Embryos and their placentae were recovered by Caesarean section at the day of birth (E19.5). **b**, Average placental weights at E19.5. Error bars indicate s.e.m. $^{**}P < 0.01$. **c**, Mating scores of *Tet1*$^{+/-}$ male × wild-type female (×Het) and *Tet1*$^{-/-}$ male × wild-type female (×KO) mice. Black dots indicate the number of pups for each litter recovered by Caesarean section at E19.5. Red lines indicate the mean litter size. **d**, Representative image of E10.5 *Tet1* paternal^{KO} embryos from the mating of wild-type female with *Tet1* knockout male mice. The dotted oval indicates morphologically abnormal embryos. **e**, Left: E9.5 paternal^{KO} embryos recovered from a single litter. Dotted oval indicates small embryos whose placentae are morphologically abnormal. Right: placentae of the corresponding embryos shown in the left panel. The red rectangle indicates morphologically abnormal placentae. **f**, Summary of embryonic abnormality. Asterisk indicates the numbers of morphologically abnormal embryos (E10.5) or placentae (E9.5). **g**, qRT–PCR analysis of selected imprinted genes in each of the E9.5 embryos from two litters (paternal^{KO} 1 and paternal^{KO} 2) are shown. Arrows indicate the samples showing marked change in expression level. The Ct values are normalized to the expression level of Gapdh.

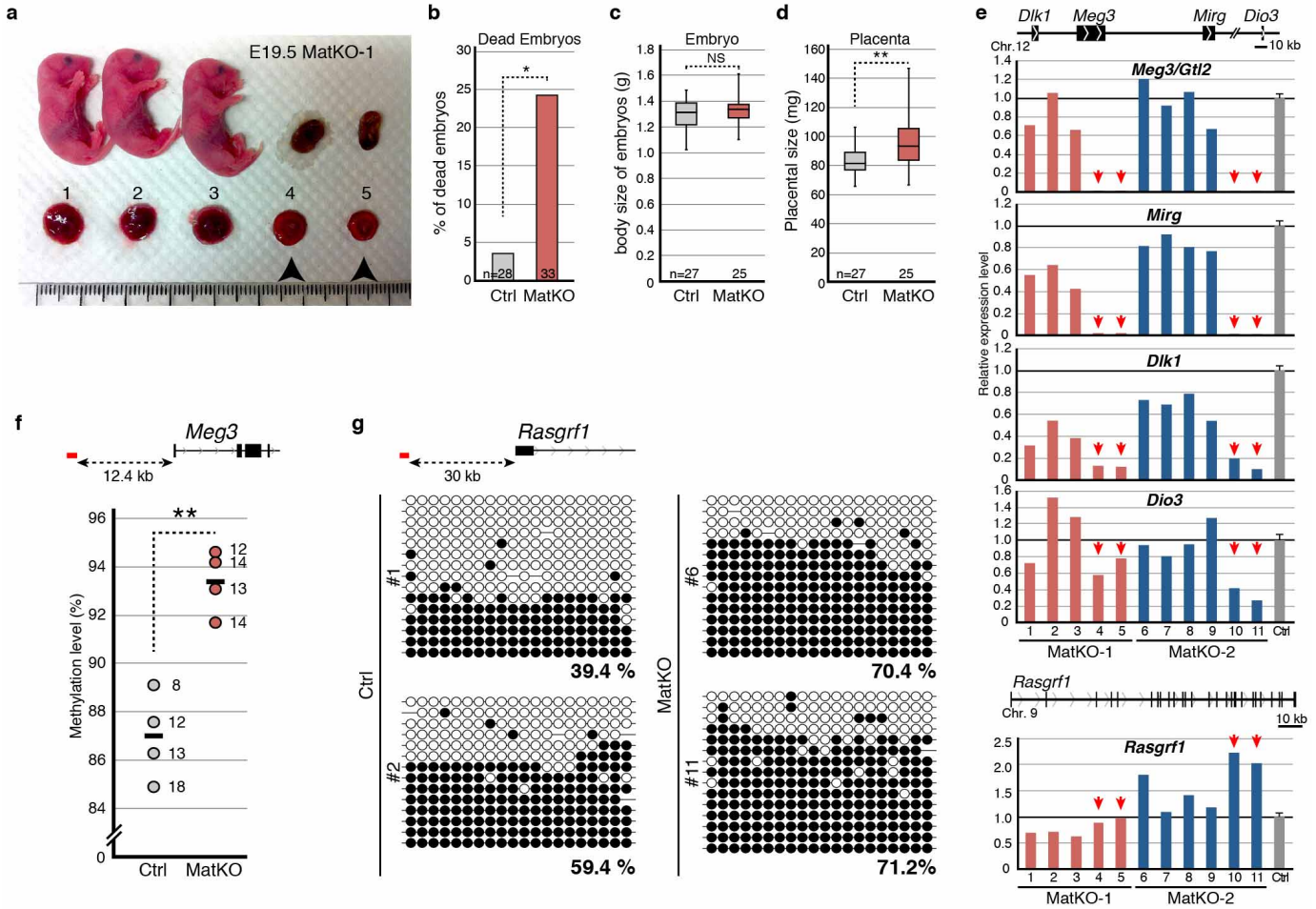

Extended Data Figure 10 | Defects in embryonic development and genomic imprinting in E19.5 *Tet1* maternal knockout embryos and placentae. **a**, Representative image of embryos and placentae from a single litter of E19.5 *Tet1* maternal^{KO} mice. Arrowheads indicate dead embryos whose placentae were morphologically normal. **b**, The ratio of dead embryos with relatively normal placentae. **c**, **d**, Box blot representation of the weight of embryos (**c**) and placentae (**d**). Middle lines in the coloured boxes indicate the medians, box edges indicate the 25th/75th percentiles, and whiskers the 0th/100th percentiles. **e**, qRT–PCR analysis of paternally imprinted genes in *Tet1* maternal^{KO} placentae. Arrows indicate the placentae whose embryos were found dead *in utero*, as indicated by arrowheads in **a**. The average value of control embryos ($n = 19$) is set as 1. Error bars indicate s.e.m. **f**, BS-seq revealed hypermethylation in *Tet1* maternal^{KO} mice in the IG-DMR locus. Note that methylation level in *Tet1* maternal^{KO} mice was significantly higher than in control mice, although IG-DMR gained methylation during placental development. Each dot represents the methylation level of each placenta. The numbers next to each dot indicate the number of clones sequenced. The average methylation levels are indicated by horizontal lines. The analysed region is indicated by a red line at the top of the diagram. **g**, BS-seq analysis of *Rasgrf1* DMR of E19.5 placentae. The analysed region is indicated by a red line at the top of the diagram. Each CpG is represented by a circle with methylation and non-methylation represented by open and filled circles, respectively. The percentages of DNA methylation are indicated. $^{*}P < 0.05$. $^{**}P < 0.01$.

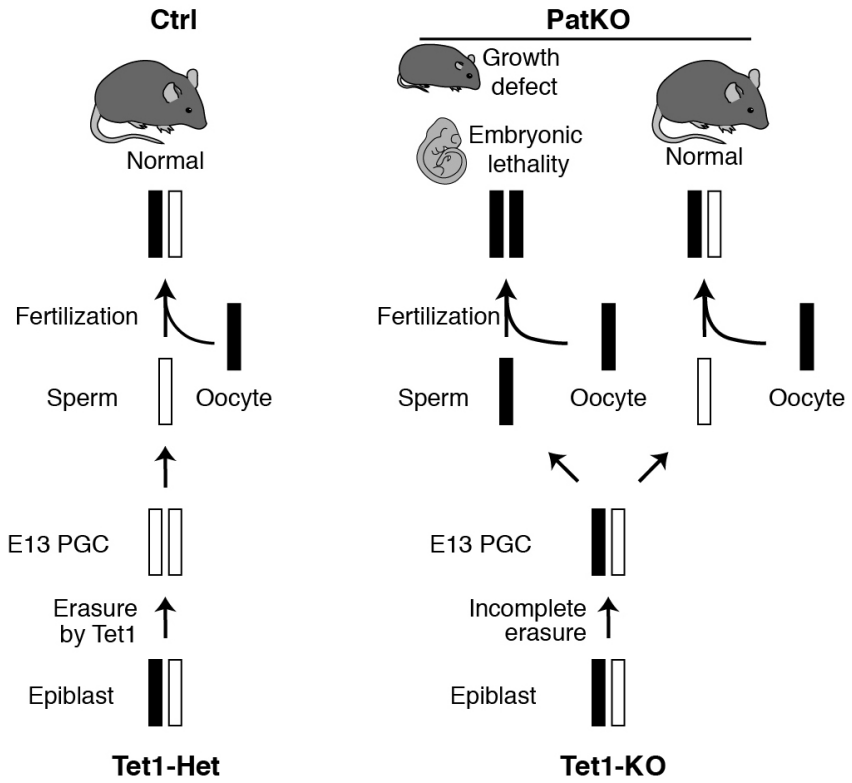

Extended Data Figure 11 | Model explaining *Tet1* paternal knockout phenotypes, using one maternal germline DMR as an example. Black and white bars represent methylated and unmethylated state, respectively. In the control, the maternal allele is completely demethylated through Tet1-mediated imprinting erasure during PGC reprogramming. However, in *Tet1* knockout PGCs, DMRs fail to be demethylated. The remaining methylation in the maternal allele is inherited to the next generation, which leads to imprinting defects.